DISCRETE AND CONTINUOUS
DYNAMICAL SYSTEMS–SERIES B
Volume ?, Number 0?, ? 2003

Website: http://AIMsciences.org

pp. 1–14

STATISTICAL EQUILIBRIUM OF THE COULOMB/ VORTEX GAS ON THE UNBOUNDED 2-DIMENSIONAL PLANE

Syed M. Assad

Department of Physics
National University of Singapore
Singapore

Chjan C. Lim

Department of Mathematical Sciences
Rensselaer Polytechnic Institute
Troy, NY 12180 USA

Dedicated to the memory of Julian D. Cole

Abstract. This paper presents the statistical equilibrium distributions of single-species vortex gas and cylindrical electron plasmas on the unbounded plane obtained by Monte Carlo simulations. We present detailed numerical evidence that at high values of $\beta > 0$ and $\mu > 0$, where β is the inverse temperature and μ is the Lagrange multiplier associated with the conservation of the moment of vorticity, the equilibrium vortex gas distribution is centered about a regular crystalline distribution with very low variance. This equilibrium crystalline structure has the form of several concentric nearly regular polygons within a bounding circle of radius R. When $\beta \sim O(1)$, the mean vortex distributions have nearly uniform vortex density inside a circular disk of radius R. In all the simulations, the radius $R = \sqrt{\beta\Omega/(2\mu)}$ where Ω is the total vorticity of the point vortex gas or number of identical point charges. Using a continuous vorticity density model and assuming that the equilibrium distribution is a uniform one within a bounding circle of radius R, we show that the most probable value of R scales with inverse temperature $\beta > 0$ and chemical potential $\mu > 0$ as in $R = \sqrt{\beta\Omega/(2\mu)}$.

1. **Introduction.** The equilibrium point vortex gas distribution of a finite number of point vortices in thermal contact with an energy reservoir can be described completely by a Gibbs canonical partition function. Interest in this problem has increased recently in view of its links to random matrix theory and to the distribution of zeroes of the Riemann zeta function [6], [4]. Furthermore, plasma physicists have been interested in understanding the statistical properties of the cylindrical electron plasmas with a view towards the problem of magnetic confinement [2]. Some of the previous works have touched on a possible virial theorem for this problem. Another approach used the mean field equations which are nonlinear elliptic PDEs and found a relationship for the radius R of the plasma which is related but different from that in this paper.

The approach in this paper differs fundamentally in the sense that a mean field approximation is not taken. Indeed it is not valid to take a mean field approach here because in this problem, we are not dealing with a fixed bounded flow domain for which a nonextensive thermodynamic or mean field limit exists. The determination of flow domains is part of the problem. The vortex gas is in principle free to occupy

the whole plane subject to certain conserved quantities such as the moment of vorticity.

The expression of the partition function for this problem remains unsolved. So to study the equilibrium point vortex gas distributions, an alternative statistical method based on the Monte Carlo algorithm, is used here. Except for the assumption of a continuous vorticity distribution in section 2 which allow the derivation of an analytical result for the radius R, no approximations of the point vortex interactions will be used in any of the numerical simulations in this paper. Since the mean field approach is not taken, we should be able to evaluate the role of fluctuations in the equilibrium statistics of the point vortex gas, using the Monte-Carlo method.

The interaction of N point vortices on the plane is governed by the logarithmic Hamiltonian

$$H_N(\vec{s}) = -\sum_{j<k}^{N} \lambda_j \lambda_k \ln|z_j - z_k|$$

where $z_j \in C$ is the position of vortex j in the complex plane, λ_j represents the strength of the j-th vortex and $\vec{s}$ represents the state of the entire system (vortex strengths and positions of all vortices). The Hamiltonian involves a sum taken over all possible vortex pairs.

Rotational invariance of H_N implies that

$$\Gamma(\vec{s}) = \sum_{j=1}^{N} \lambda_j |z_j|^2$$

is a first integral of motion. The remaining first integrals are the linear momenta

$$\Phi(\vec{s}) = \sum_{j=1}^{N} \lambda_j z_j \in C$$

associated with the translational invariance of H_N. These can be neglected in a statistical mechanics formulation for the point vortex gas by virtue of the fact that a judicious choice of the origin of the coordinate system eliminates them.

The potential energy of 2-D Coulombic interactions in a long cylindrical electron plasmas is also given by H_N which means that the equilibrium statistical mechanics of the plasma is identical to that of the single species vortex gas [3], [2]. This equilibrium statistical mechanics is completely prescribed by the partition function [1]

$$Z(\beta, \mu) = \int_{R^2} dz_1 ..... \int_{R^2} dz_N \exp(-\beta H) \exp(-\mu \Gamma) \tag{1}$$

where β and μ are the Lagrange multipliers associated with the energy and moment of vorticity respectively. In other words, β is the inverse of a temperature for the vortex gas and μ is a chemical potential. The parameter μ is related to the Larmor frequency in the electron plasma [3] [2]. When all λ_j are positive, the partition function Z is bounded only if $\mu > 0$.

Then for a fixed β, μ and N, the probability of an arbitrary state $\vec{s}$ is given by

$$P(\vec{s}) = \frac{1}{Z} \exp[-\beta H(\vec{s}) - \mu \Gamma(\vec{s})]$$

The positive-definiteness of Γ implies that it effectively bounds the region in which the vortex gas density is nonzero. For $\beta > 0$, the form of H implies that the most probable macrostate or vortex gas distribution is one where the vortices are widely separated within the constraint imposed by $\mu > 0$.

Although the partition function Z is unknown for most values of β and μ, Ginibre [5] derived an exact solution for the one-particle reduced distribution function

$$G_1^N(z) = \exp(-|z|^2) \sum_{k=0}^{N-1} \frac{|z|^{2k}}{k!} \to 1 \text{ as } N \to \infty \tag{2}$$

when $\beta = 2$ and $\mu = 1$. His method was based on the Wigner-Dyson model of the statistics of the spectra of random matrices. From G_1^N we infer the distribution of a point vortex gas of N identical vortices in the canonical ensemble at an inverse temperature $\beta = 2$ and chemical potential $\mu = 1$ has the form of a nearly uniform density in a disk of radius $R \sim \sqrt{N}$ and exponentially decaying density outside.

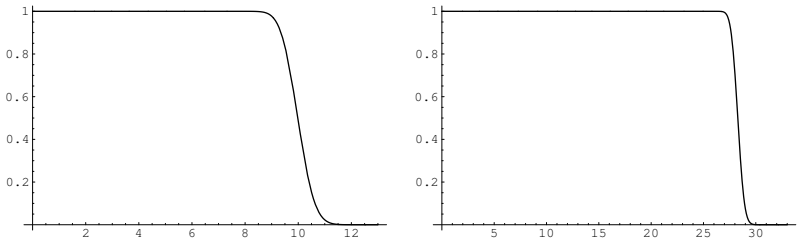

$G_1^{100}(|z|)$ $G_1^{800}(|z|)$

FIGURE 1. One-particle reduced distribution function from Ginibre's exact solution. It is nearly constant for $r < \sqrt{N}$ and drops to zero for $r > \sqrt{N}$.

Our main result is that for other order one values of β and μ, we have a similar result, that is the vortex density is almost constant in a disk of radius $R \sim \sqrt{N}$ and drops exponentially to zero outside. The exponential drop becomes sharper when the value of β and μ increases. The Monte - Carlo simulations strongly suggests the relationship $R = \sqrt{\beta\Omega/(2\mu)}$ between the radius of the support for the nearly uniform vortex density function, the total vorticity or charge Ω and the Lagrange multipliers in the problem.

In section 2 below, we present a derivation of this radius relationship using a continuous vortex density model and assuming that the equilibrium distribution is a uniform density inside a circular disk of some radius R. In Lim and Assad [7], it was shown by variational methods that the uniform vortex density of $2\mu/(\pi\beta)$ inside a disk of radius $R = \sqrt{\beta\Omega/(2\mu)}$ attains the lowest augmented energy in the Hilbert space of all bounded positive vortex density functions including non-axisymmetric ones. Keeping in mind that the continuous vorticity model differs from the point vortex gas in many ways, it is surprising that such an exact comparison between theory and numerics could be found.

Moreover, we found that the ground state (lowest energy state) for a vortex distribution can be obtained by a Monte Carlo simulation with a large value of β and μ. This ground state is a regular crystalline vortex distribution of concentric polygons inside a disk of radius $R = \sqrt{\beta\Omega/(2\mu)}$. It is beyond our understanding

at this point why the crystalline ground state is again contained precisely within a bounding circle of radius $R = \sqrt{\beta\Omega/(2\mu)}$. It is even more surprising why the crystalline ground state which is clearly a non-uniform vortex distribution should obey the same radius scaling relationship.

Part of the results in this paper is devoted to understanding the role of fluctuations in the equilibrium statistics of the vortex gas. We will present numerical results suggesting that the relative size of fluctuations decrease as the inverse temperature $\beta > 0$ increases. Using an exact factorization of the partition function derived in Assad and Lim [8], we derive closed form expressions for the mean and variance of the moment of vorticity Γ and compare them with the numerical values obtained by Monte-Carlo simulations. We also provide evidence that at $\beta \sim O(1)$ fluctuations is responsible for the nearly uniform vortex density found inside the bounding radius R.

2. **Derivation of the most probable radius.** For a fixed value of β and μ, consider instead of N point vortices, a continuous vorticity distribution defined by a vortex density function $\rho(r,\theta)$. Moreover consider such a vortex density $\rho(r)$ that depends only on r. We wish to find a unique value of R that maximizes the Gibbs factor $\exp(-\beta H - \mu\Gamma)$. We have the moment of vorticity

$$\begin{aligned}\Gamma &= \int_D \rho(r) r^2 \, d\vec{r} \\ &= 2\pi \int_0^\infty \rho(r) r^3 \, dr \ , \end{aligned} \tag{3}$$

and the kinetic energy of flow

$$\begin{aligned} H &= -\frac{1}{2}\int_D\int_D \rho(r_1)\rho(r_2)\log|\vec{r_1}-\vec{r_2}|\, d\vec{r_1}\, d\vec{r_2} \\ &= -\int_0^\infty dr_1 \int_0^{r1} dr_2 \int_0^{2\pi} d\theta_1 \int_0^{2\pi} d\theta_2 r_1 r_2 \rho(r_1)\rho(r_2) \\ &\quad \times \log\left[{r_1}^2 + {r_2}^2 - 2r_1 r_2\cos(\theta_1-\theta_2)\right]^{1/2} \\ &= -\frac{2\pi}{2}\int_0^\infty dr_1 \int_0^{r1} dr_2 \int_0^{2\pi} d\theta_1 r_1 r_2 \rho(r_1)\rho(r_2) \\ &\quad \times \log\left[{r_1}^2 + {r_2}^2 - 2r_1 r_2\cos(\theta_1)\right] \\ &= -\pi\int_0^\infty dr_1 \int_0^{r1} dr_2 r_1 r_2 \rho(r_1)\rho(r_2) \\ &\quad \times 2\pi \log\left(\frac{{r_1}^2 + {r_2}^2 + \sqrt{({r_1}^2+{r_2}^2)^2 - 4{r_1}^2{r_2}^2}}{2}\right) \\ &= -4\pi^2\int_0^\infty dr_1 \int_0^{r1} dr_2 r_1 r_2 \rho(r_1)\rho(r_2)\log(r_1) \ . \end{aligned} \tag{4}$$

If we consider the specific case of a uniform vortex density $\frac{N}{\pi R^2}$ of total circulation N within a disk D_R of radius R and zero density outside the disk, we get

$$\begin{aligned}\Gamma &= \frac{N}{\pi R^2}\int_0^R r^3 dr \\ &= \frac{N}{\pi R^2}\times 2\pi \times \frac{R^4}{4} \\ &= \frac{NR^2}{2}\,, \end{aligned} \tag{5}$$

and

$$\begin{aligned} H &= -4\pi^2\frac{N^2}{\pi^2 R^4}\int_0^R dr_1 \int_0^{r_1} dr_2 r_1 r_2 \log(r_1) \\ &= -\frac{4N^2}{R^4}\int_0^R dr_1 \frac{{r_1}^3}{2}\log(r_1) \\ &= -\frac{N^2}{8}(4\log R - 1)\,. \end{aligned}$$

In order to maximize the Gibbs factor, we need

$$\begin{aligned} \frac{\partial}{\partial R}\exp\left[-\beta H(R,N) - \mu\Gamma(R,N)\right] &= 0 \\ \frac{\partial}{\partial R}\left[-\beta H(R,N) - \mu\Gamma(R,N)\right] &= 0 \end{aligned}$$

which leads to

$$-\beta\frac{N^2}{2R} = -\mu N R$$

and thus the relationship we want, namely

$$R^2 = \frac{\beta N}{2\mu}.$$

Since the total vorticity $\Omega = N\lambda$ where $\lambda = 1$ is the vortex strength of the N identical charges we get

$$R^2 = \frac{\beta\Omega}{2\mu}. \tag{6}$$

Keeping in mind that the continuous vorticity model differs from the singular point vortex or Coulomb gas problem, the exact match between the expression (6) and the numerical results that we present below is remarkable.

Digressing a little, equation (4) can be written as

$$H = -2\pi\int_0^\infty dr_1 r_1 \rho(r_1)\log(r_1)\Omega(r_1)$$

where $\Omega(r_1) = 2\pi\int_0^{r_1} r_2\rho(r_2)dr_2$ is the total circulation inside a disk of radius r_1. This says that for a radially symmetric distribution, the interaction energy of an annular ring at radius r_1 of width dr_1 with the rest of the system is equivalent to the interaction energy of the same ring with a point vortex of circulation $\Omega(r_1)$ at the origin. The vortex density outside r_1 have no effect on the interaction energy.

3. **The Monte Carlo algorithm.** A Monte Carlo algorithm following the Metropolis rule is used to generate a Markov chain of states $\{\vec{s_i}\}$. A sweep in the Metropolis rule consist of N proposed displacements, where N is the number of vortices. The vortices were subjected to a proposed displacement in a fixed order. A proposed displacement consist of moving the vortex by a random fraction of a predetermined small distance, in a random direction. The change in the augmented energy $\Delta E = \Delta H + (\mu/\beta)\Delta\Gamma$ that this proposed move would cause was then calculated. The move is then accepted or rejected based on a randomly chosen number r uniformly distributed on $(0, 1)$. If $r < \exp(-\beta\Delta E)$, the move is be accepted. Otherwise the move is rejected. The process was then repeated for the next vortex.

Our experiments involve positive β, and the Metropolis rule will accept all moves that results in a lowered augmented energy. A move that results in a higher augmented energy might still be accepted based on the value of β as well as the random number r. We allow the vortices to equilibrate with the energy reservoir by allowing a preselected number of sweeps (20000) to pass. An ensemble of states were then gathered by sampling the distribution after every 50 sweeps for a total of 100000 sweeps.

4. **Numerical results from the Monte Carlo algorithm.** In this section, we present the statistical results obtained using the Monte Carlo algorithm.

Figure 2 were obtained from Monte Carlo simulations at high values of β and μ, for different number of vortices N ranging from 50 to 1000. The strength of each vortex has been set to unity and R_{max} is the distance of the furtherest vortex from the origin.

This figure shows that ${R_{max}}^2$ is proportional to the total vortex strength N. The gradient of the three graphs are all proportional to β/μ, and the proportionality constant being $1/2$ in each case. This fits the result of equation (6) for the continuous uniform distribution, $R^2 = \beta\Omega/(2\mu)$.

Figures 3 - 9 were obtained from four Monte Carlo runs with the total number of vortices $N = 800$. The strength of each vortex were once again set to one. The vortices were allowed to equilibrate with the kinetic and moment of vorticity reservoirs in the first 20000 sweeps. Subsequently, the vortex distribution was sampled after every 50 sweeps for a total of 100000 sweeps.

In each of these four experiments, the ratios of β and μ have been kept constant. But the magnitude of β and μ were increased by a factor of 1000 in each subsequent experiment.

4.1. **Vortex distribution after** 100000 **sweeps.** Figure 3 shows the final vortex distributions after 100000 sweeps. In figure (a), when the value of β and μ is low, we see a disordered distribution. The circle of radius $R = \sqrt{\beta N/(2\mu)} = \sqrt{200}$ was drawn to aid visual comparison between the figures.

In figure (b), when the values of β and μ increases to 1 and 2 respectively, more than 90% of the vortices are now concentrated inside the circle. The density distribution inside this circle is not uniform.

At even higher values of β and μ as in figures (c) and (d), the distribution now becomes more ordered. But the size of the region occupied by the vortices remains around the same. Here, all of the vortices fall inside the circle, and they have an ordered crystalline distribution. In these distributions, we expect that the vortices are spaced maximally apart inside a finite disk, so as to allow for the lowest possible kinetic energy.

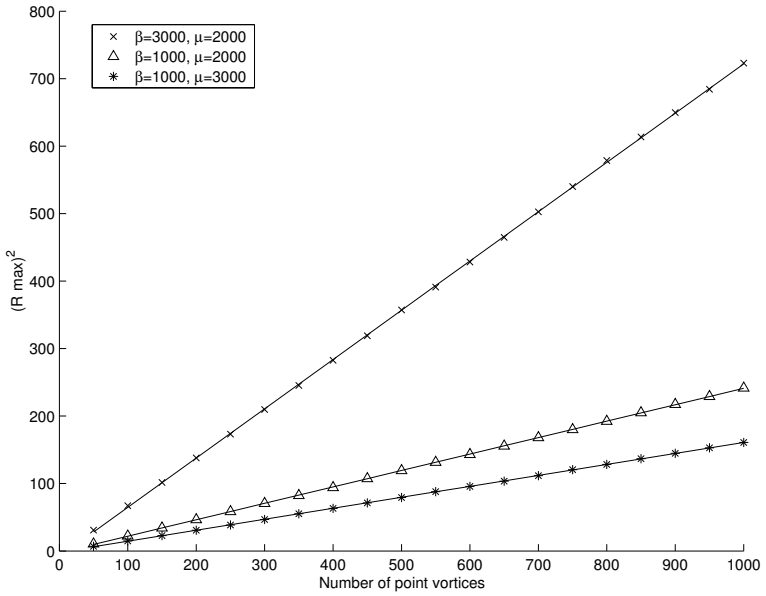

FIGURE 2. For large β and μ, the square of the distance of the furthest point vertex from the origin is directly proportional to the number of vortices.

4.2. **Radial distribution.** The radial density $rad(r)$ for a vortex distribution is defined as the number of vortices that falls in a unit annulus element centered at the origin, with central radius r.

Figure 4 shows the radial density for the vortex distributions at sweep 100000 for $N = 800$. We had used annuli of width 0.2 to cover the region occupied by the vortices. The radial density for a distribution was then obtained by diving the number of vortices in an annulus by the area of the annulus.

To get the mean radial density, we took the average of all the radial densities in the ensemble. In these calculations for the mean radial density, we covered the whole region occupied by the vortices by annuli of width 0.05.

Figure 5 shows the mean radial vortex density distribution. In figure (a), when β and μ is low, the particle density decays slowly with r. There is a low mean density of 0.4 near the origin. This drops gradually to zero when the radius reaches 60.

For $\beta = 1$ and $\mu = 2$, we see a nearly constant vortex density around 1.3 for $r < 13$. At $r > 13$, the vortex density drops rapidly until it reaches zero at $r = 16$. The shape of the distribution is similar to the exact density distribution Ginibre obtained for $\beta = 2$ in figure 1. And the radius at which the density drops to approximately half its maximum value is given by $R = \sqrt{\beta N/(2\mu)}$.

As the magnitude of β and μ increases further, the drop in particle density becomes even sharper as seen in figures (c) and (d). The radial density have sharp peaks at several values of r and a near zero density in between some of these peaks.

At high values of β and μ, the probability of the Metropolis algorithm accepting a proposed move that results in a higher augmented energy becomes very small. So most of the accepted move would result in a lower augmented energy state. When the Metropolis algorithm reaches a low augmented energy state, the probability that

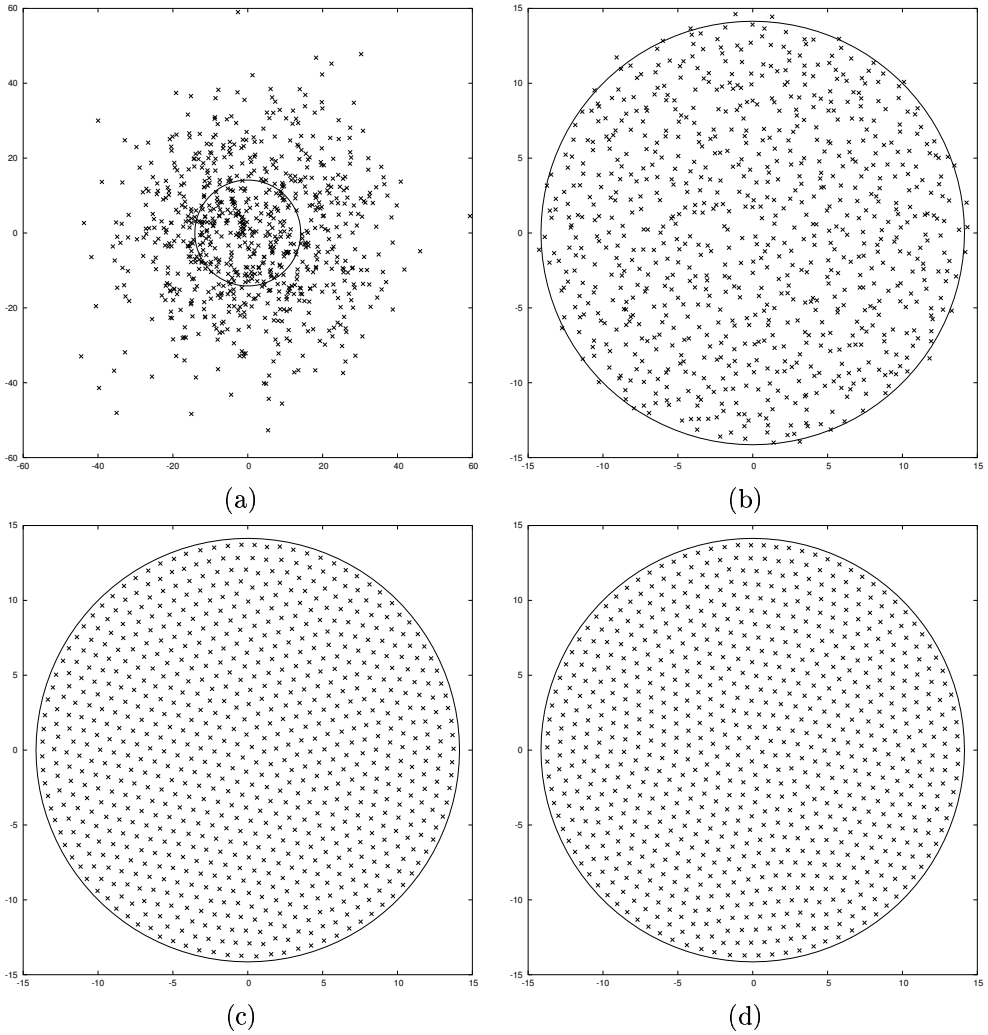

FIGURE 3. Vortex distribution on the unbounded plane after 100000 sweeps for $N = 800$ at (a) $\beta = 0.001$ and $\mu = 0.002$, (b)$\beta = 1$ and $\mu = 2$, (c)$\beta = 1000$ and $\mu = 2000$ and (d)$\beta = 1000000$ and $\mu = 2000000$.

it would deviate far from this state is low. As a result, the algorithm will produce an ensemble of states that consists of vortex distributions that are very similar to each other, and each having the same low augmented energy. In these distributions, the vortices hardly change their positions, and as a result each sampling measures the same radial distributions over and over again.

4.3. **Mean angular distribution.** The angular density $ang(\theta)$ for a vortex distribution is defined as the number of vortices falling inside an infinite sector element of angular width $d\theta$ bisected by the half-line θ and centered at the origin times $2\pi/(Nd\theta)$. The factor $2\pi/(Nd\theta)$ would normalize the density at each θ to one. In our calculations we covered the plane by sectors of width 0.5 degrees. To get

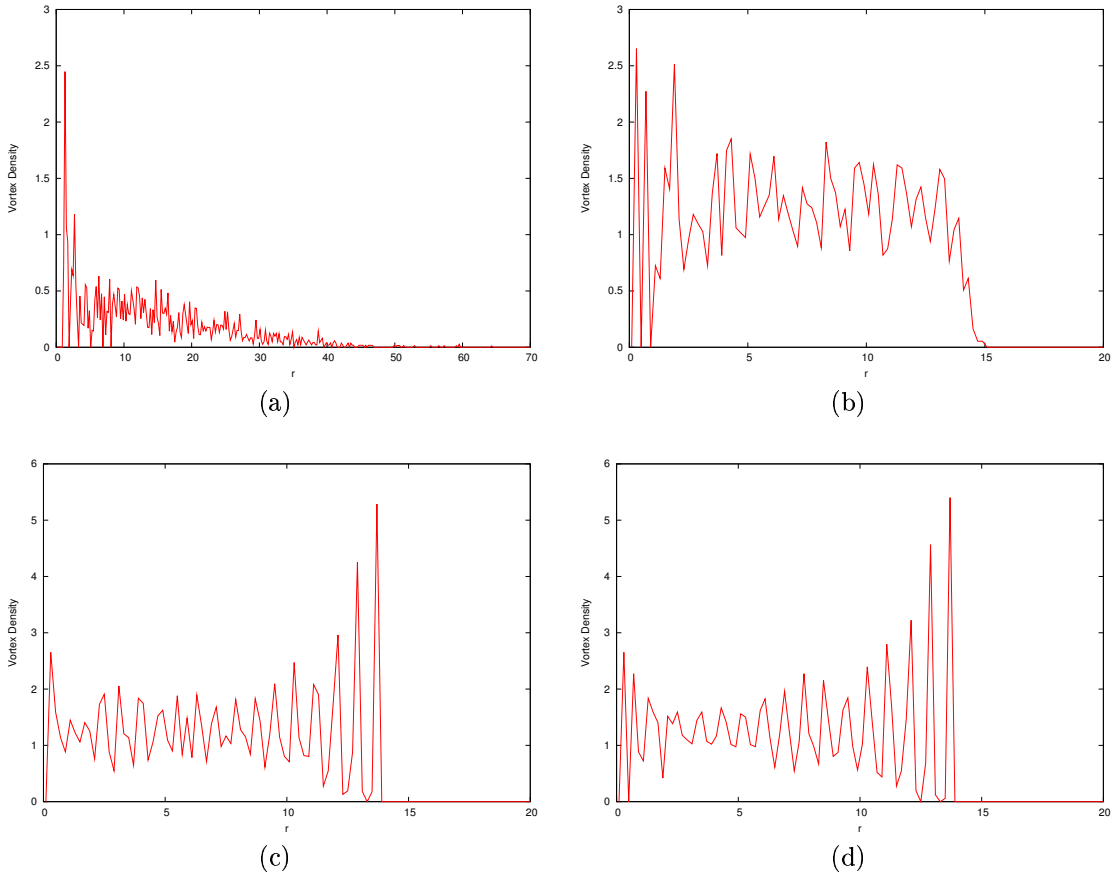

FIGURE 4. Radial density of the vortex distribution after 100000 sweeps for $N = 800$ at (a) $\beta = 0.001$ and $\mu = 0.002$, (b)$\beta = 1$ and $\mu = 2$, (c)$\beta = 1000$ and $\mu = 2000$ and (d)$\beta = 1000000$ and $\mu = 2000000$.

the mean angular density, we took the average of all the angular densities in the ensemble.

Figure 6 shows the mean angular particle density. It fluctuates around 1 in the figures (a) and (b) as expected. Since rotating a distribution would not change its augmented energy, we expect that the equilibrium vortex distribution would be isotropic and not have any angular dependence. However in figures (c) and (d), where the magnitudes of β and μ are large, the fluctuations are larger. This is due to a regular vortex distribution at finite N that does not change very much after each sweeps.

4.4. **Mean and variations of kinetic energy and the moment of vorticity.** The values of the kinetic energy H, moment of vorticity Γ and the augmented energy E at each sampled sweep are given in figures 7, 8 and 9 respectively.

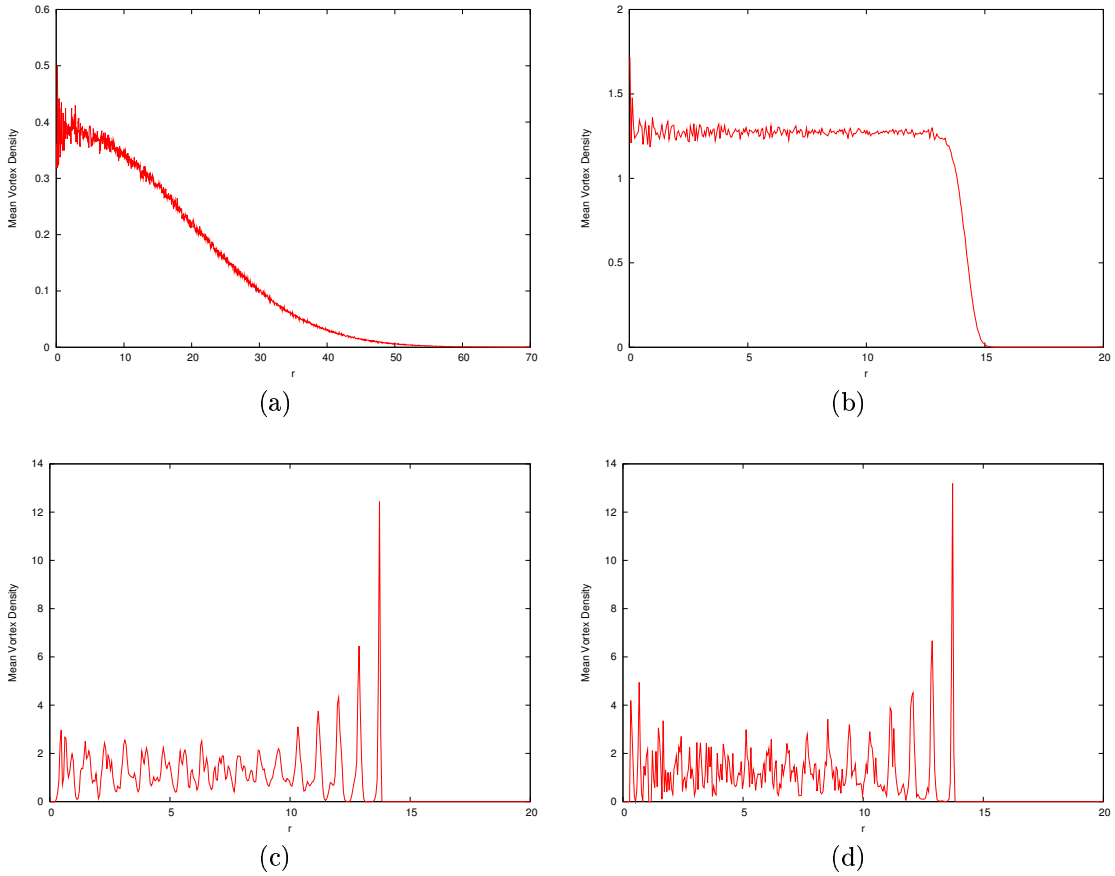

FIGURE 5. Mean radial density for $N = 800$ at (a) $\beta = 0.001$ and $\mu = 0.002$, (b)$\beta = 1$ and $\mu = 2$, (c)$\beta = 1000$ and $\mu = 2000$ and (d)$\beta = 1000000$ and $\mu = 2000000$.

In figure 9(d), we see that the augmented energy is still decreasing after the first 20000 equilibration sweeps. In general, the number of sweeps needed for the vortices to equilibrate is larger for higher values of β and μ.

The mean value kinetic energy were calculated by taking the simple average of the kinetic energies of all the sampled distribution after 20000 sweeps have elapsed:

$$\langle H_{MC} \rangle = \frac{1}{T} \sum_{i=1}^{T} H_N(\vec{s_i}),$$

where $\vec{s_i}$ is the sampled states and T is the total number of sampled states. The variance of the kinetic energy was evaluated using the formula:

$$\text{Variance}(H_{MC}) = \frac{T}{T-1} \left(\langle H(\vec{s})^2 \rangle - \langle H(\vec{s}) \rangle^2 \right).$$

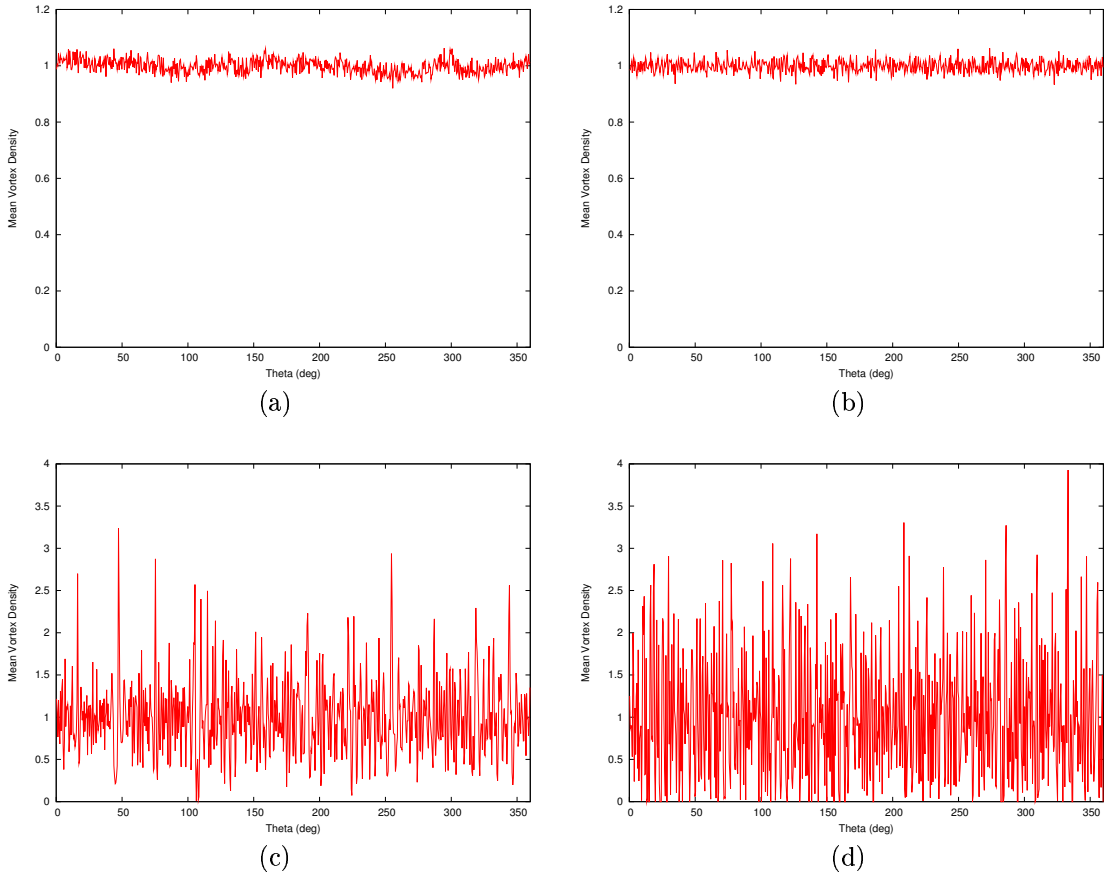

FIGURE 6. Mean angular density for $N = 800$ at (a) $\beta = 0.001$ and $\mu = 0.002$, (b)$\beta = 1$ and $\mu = 2$, (c)$\beta = 1000$ and $\mu = 2000$ and (d)$\beta = 1000000$ and $\mu = 2000000$.

The mean and variance of H, Γ and E are shown in table 1. The values of H and Γ tends to decrease as the magnitude of β and μ increase. Also at high β and high μ, the variance in H and Γ is low.

5. **Moment of vorticity - mean and variance analysis.** For completeness we include a result from Assad and Lim [8] on the chemical potential or μ - dependence of the N particle partition function Z, namely

$$Z(\beta, \mu) = \mu^{\frac{N}{4}(4+\beta N-\beta)} F(\beta, N)$$

where $F(\beta, N)$ is some function that does not depend on μ. From this expression, we derive the expected value of the moment of vorticity

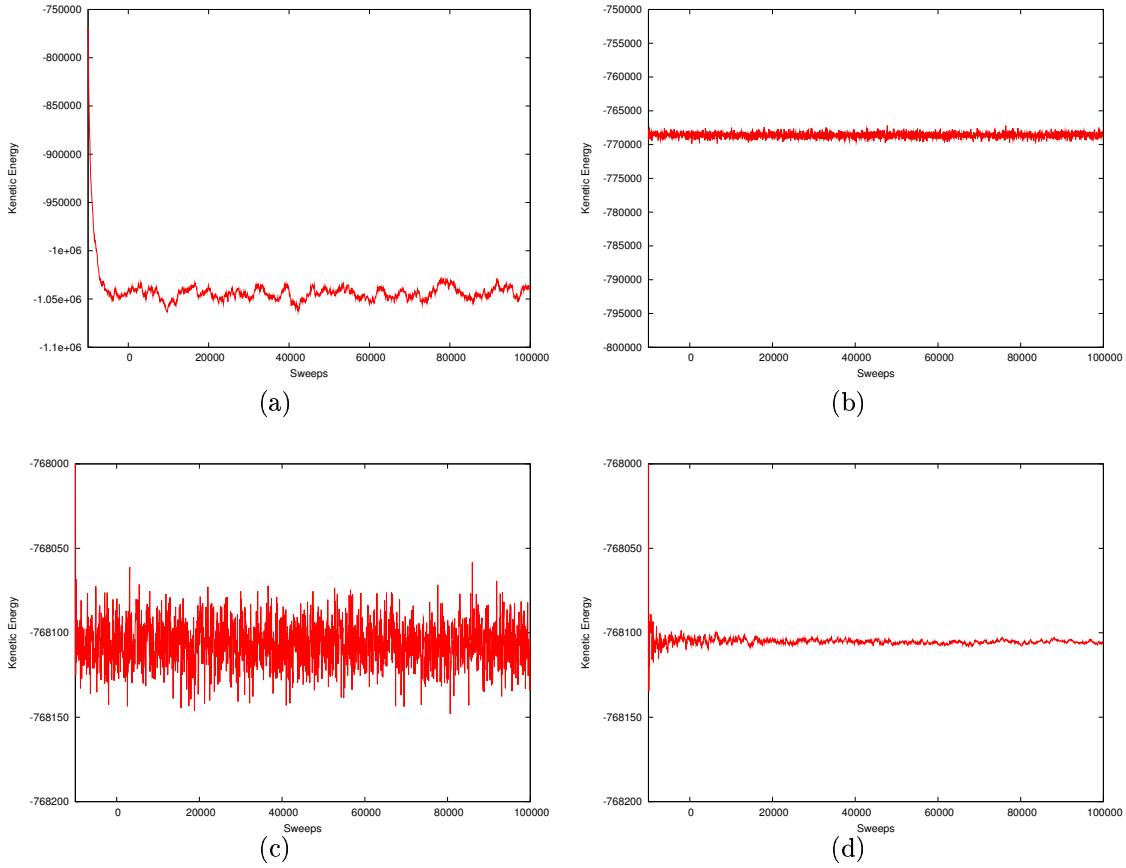

FIGURE 7. Energy for $N = 800$ at (a) $\beta = 0.001$ and $\mu = 0.002$, (b)$\beta = 1$ and $\mu = 2$, (c)$\beta = 1000$ and $\mu = 2000$ and (d)$\beta = 1000000$ and $\mu = 2000000$.

	$\beta = 10^{-3}$ $\mu = 2 \times 10^{-3}$	$\beta = 1$ $\mu = 2$	$\beta = 10^{3}$ $\mu = 2 \times 10^{3}$	$\beta = 10^{6}$ $\mu = 2 \times 10^{6}$
$\langle H \rangle$	-1.0442e06	-7.6861e05	-7.6811e05	-7.6811e05
Variance(H)	3.4293e07	1.6009e05	163.42	1.3744
$\langle L \rangle$	4.8420e05	8.0301e04	7.9901e04	7.9900e04
Variance(L)	3.1423e08	4.0317e04	40.831	0.31415
$\langle E \rangle$	-7.5839e04	-6.0801e05	-6.0830e05	-6.0831e05
Variance(E)	8.8735e08	173.98	0.013725	0.063750

TABLE 1. Mean and variance of the kinetic energy, moment of vorticity and the augmented energy for the unbounded particle Monte Carlo simulations.

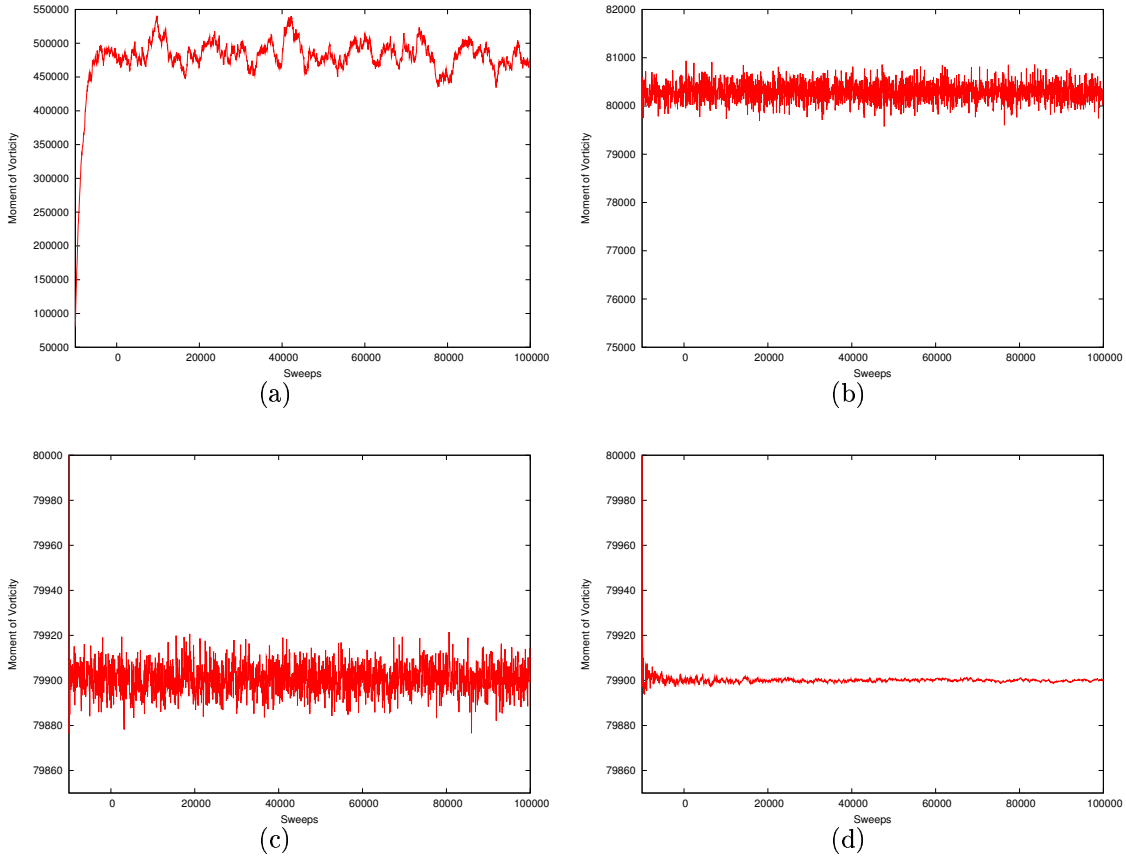

FIGURE 8. Moment of vorticity for $N = 800$ at (a) $\beta = 0.001$ and $\mu = 0.002$, (b)$\beta = 1$ and $\mu = 2$, (c)$\beta = 1000$ and $\mu = 2000$ and (d)$\beta = 1000000$ and $\mu = 2000000$.

$$\begin{aligned} \langle \Gamma \rangle &= -\frac{\partial}{\partial \mu} \log(Z_N) \\ &= \frac{N}{4\mu}(4 + \beta N - \beta) \end{aligned}$$

as well as its variance

$$\begin{aligned} \text{Variance}(\Gamma) &= \frac{\partial^2}{\partial \mu^2} \log(Z_N) \\ &= \frac{N}{4\mu^2}(4 + \beta N - \beta) \end{aligned}$$

Table 2 compares the theoretical expressions for the mean and variance of the moment of vorticity with the numerical values obtained from the Monte Carlo simulations for $N = 800$. The values stated for the Monte Carlo simulations were

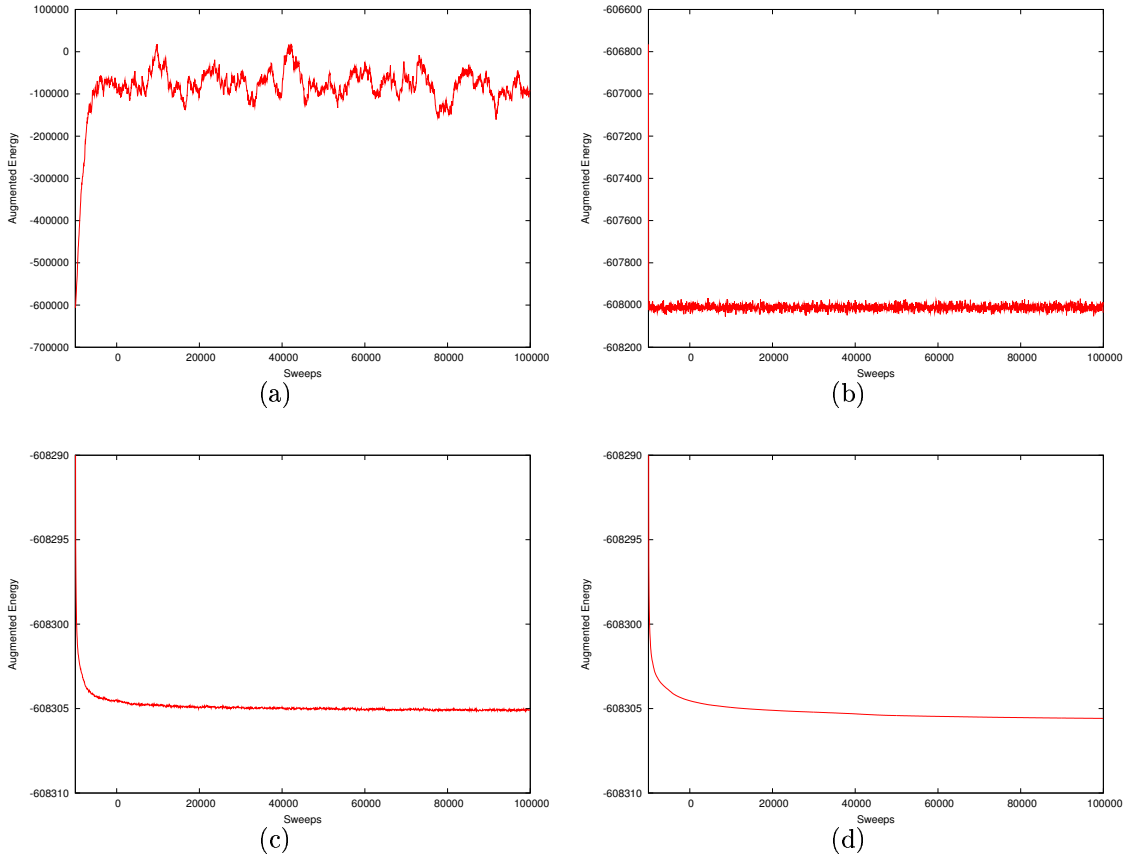

FIGURE 9. Augmented energy for $N = 800$ at (a) $\beta = 0.001$ and $\mu = 0.002$, (b)$\beta = 1$ and $\mu = 2$, (c)$\beta = 1000$ and $\mu = 2000$ and (d)$\beta = 1000000$ and $\mu = 2000000$.

obtained by running 20000 sweeps to allow the vortices to equilibrate; and then sampling the distributions at every 50 sweeps for 100000 sweeps.

β	μ	$\langle\Gamma_{MC}\rangle$	$\langle\Gamma\rangle$	Variance(Γ_{MC})	Variance(Γ)
10^{-3}	2×10^{-3}	4.8420e05	4.7990e05	3.1423e08	2.3995e08
1	2	8.0301e04	8.0300e04	4.0317e04	4.0150e04
10^3	2×10^3	7.9901e04	7.9900e04	40.831	39.950
10^6	2×10^6	7.9900e04	7.9900e04	0.31415	0.03995
1	2×10^3	80.303	80.300	0.039146	0.040150
10^3	2	7.9900e07	7.9900e07	4.0893e07	3.9950e07

TABLE 2. Comparison between the theoretical and Monte Carlo results of the mean and variance moment of vorticity.

Table 2 shows that there is a good agreement between the theoretical expressions and the Monte Carlo numerical values of the mean and variance of Γ for a wide

range of values of β and μ. The only large discrepancy that we see is between the variances when $\beta = 10^6$ and $\mu = 2 \times 10^6$. This discrepancy is because for such large β and μ, the vortices have not yet equilibrated after 20000 sweeps.

6. **Concluding remarks.** The equilibrium statistics of the Coulomb gas in the plane is interesting because part of its resolution belongs to the active field of random matrix theory as Ginibre showed. Because of this connection and the further link to the zeroes of the Riemann zeta function, the statistical properties of the vortex gas may turn out to be useful in contemporary efforts of mathematicians.

Acknowledgment

This work was partially supported by a research grant at the National University of Singapore.

REFERENCES

[1] A. J. Chorin, *Vorticity and Turbulence,* Springer-Verlag, New York 1994.
[2] J.H. Williamson, *Statistical mechanics of a guiding center plasma,* J. Plasma Physics 17, 85-92, 1977.
[3] R.A. Smith and T.M. O'Neil, *Nonaxisymmetric thermal equilibria of a cylindrically bounded guiding center plasma or discrete vortex system,* Phys. Fluids B 2, 2961-2975, 1990.
[4] P. Deift, *Orthogonal Polynomials and Random Matrices: A Riemann-Hilbert Approach,* Courant Lecture Notes 3, AMS Press.
[5] J. Ginibre, *Statistical Ensembles of Complex, Quaternion, and Real Matrices,* J. Math Phys. 6(3), 440 - 449.
[6] M.L. Mehta, *Random Matrices,* Academic Press, New York, 1990.L. Onsager, Nuovo Cimento Suppl 1949
[7] C.C. Lim, and S.M. Assad, *A Variational Principle for the Statistical Equilibrium of the Unbounded Single-species Vortex Gas and Cylindrical Electron Plasmas*, (In preparation) 2003
[8] S.M. Assad, and C.C Lim *Partition Function of the Unbounded Single-species Vortex Gas and Cylindrical Electron Plasmas*, (In preparation) 2003

Received September 2003; revised October 2003.
E-mail address: assad@singmail.com
E-mail address: limc@rpi.edu